

# Multiscaling at Point $J$ : Jamming is a Critical Phenomenon

J. A. Drocco<sup>1</sup>, M. B. Hastings<sup>2,3</sup>, C. J. Olson Reichhardt<sup>3</sup>, and C. Reichhardt<sup>2,3</sup>

<sup>1</sup>*Department of Physics, University of Notre Dame, Notre Dame, Indiana 46656*

<sup>2</sup>*Center for Nonlinear Studies and* <sup>3</sup>*Theoretical Division, Los Alamos National Laboratory, Los Alamos, New Mexico 87545*  
(March 22, 2022)

We analyze the jamming transition that occurs as a function of increasing packing density in a disordered two-dimensional assembly of disks at zero temperature for “Point J” of the recently proposed jamming phase diagram. We measure the total number of moving disks and the transverse length of the moving region, and find a power law divergence as the packing density increases toward a critical jamming density. This provides evidence that the  $T = 0$  jamming transition as a function of packing density is a *second order* phase transition. Additionally we find evidence for multiscaling, indicating the importance of long tails in the velocity fluctuations.

PACS numbers: 45.70.-n, 64.60.Ht

There has been a surge of activity in jamming phenomena for  $T = 0$  systems such as granular materials, foams, and colloids, where jamming is defined as the onset of a nonvanishing yield stress in a disordered state [1,2]. Liu and Nagel proposed a jamming phase diagram containing three axes: temperature  $T$ , the inverse packing fraction  $1/\phi$ , and shear  $\sigma$  [1]. The system is jammed within a three-dimensional dome; above the jamming transition, the system behaves as a rigid solid. Recently O’Hern *et al.* [3] studied the area of the jamming phase diagram at  $T = \sigma = 0$  as a function of packing density  $\phi$ , and showed that a well defined sharp jamming transition appears at “Point J.” Elsewhere on the jamming phase diagram, the boundary between jammed and unjammed states is not sharp since its definition is sensitive to the experimental time scale. It was noted in Ref. [3] that, although Point J does not exist for liquids, the behavior near Point J could be relevant to the physics near the glass transition. A key question is whether Point J is a true continuous phase transition with a diverging spatial correlation length. Since the physics at Point J is non-thermal, any continuous phase transition behavior could be dominated by rare fluctuations. If this is the case, simple scaling close to the critical density may *not* occur even if there is an underlying phase transition.

Here, we consider the motion of a single disk driven through an arrangement of disks as the jamming transition is approached, a system which, as suggested in Ref. [3], should provide a direct test of the nature of the jamming transition. The reader is invited to try the following experiment: place a large collection of coins flat on a desk, so that they are almost touching. Then, push one coin and observe what other coins move. At low packing fractions  $\phi$ , the driven disk or coin occasionally contacts other disks, which can in turn contact still other disks, but the total number of disks moving is small. At a certain density  $\phi = \phi_c$ , however, the entire system must move simultaneously as a unit, and *jams*. Force chains can be observed emanating from the driven disk [4].

In these jamming problems, the tail of the particle velocity distribution  $P(v)$  at small velocities controls the

behavior of the system, since once the system enters a jammed state, with everything stopped in the thermodynamic limit, it can never exit the jammed state. The best method for characterizing the tail of  $P(v)$  is via multiscaling, which we employ in this Letter. For fixed driving force, a small  $v$  implies that a large number of other particles are dragged with the driven particle, but we can also characterize the number of particles moved by the driven particle by examining the force transmission. We will see that this measurement provides direct evidence for a diverging length scale. Our data also suggests that the jamming transition for very large systems coincides with the random close packed density.

We simulate a binary mixture of two-dimensional disks with stiff spring repulsive interactions of radius  $r_A$  and  $r_B$  at  $T = 0$  (see Fig. 1). For all the densities we consider here, we find  $\ll 1\%$  overlap in the radii as the disks interact, indicating that the spring constant is sufficiently large to provide a good approximation to hard core disks. The bimodal disk distribution, with a size ratio of  $1.4 : 1$ , is chosen to create a disordered arrangement and avoid formation of a regular lattice. We also performed simulations with a size ratio of  $1.7 : 1$  with substantially identical results. We employ overdamped dynamics such that the velocity of each disk is proportional to the force acting on it. The equation of motion for the disks is

$$\eta \mathbf{v}_i = \sum_{j \neq i} k(|\mathbf{r}_{ij}| - r_{eff}) \frac{\mathbf{r}_{ij}}{|\mathbf{r}_{ij}|} + \mathbf{f}_d. \quad (1)$$

Here  $k = 200$  is the strength of the stiff restoring spring [5],  $\mathbf{r}_{ij} = \mathbf{r}_i - \mathbf{r}_j$ , and for all but one of the disks, the external driving force  $\mathbf{f}_d = 0$ . The single driven disk (large dot in Fig. 1) has  $\mathbf{f}_d = 0.1$ . Disks only interact if they are separated by a distance smaller than the sum of their radii,  $|\mathbf{r}_{ij}| < r_{eff} = r^{(i)} + r^{(j)}$ , where  $r^{(i)}$  equals either  $r_A$  or  $r_B$ , depending on the given particle. We tested several different values of  $\mathbf{f}_d$  and chose the value small enough to minimize overlap as mentioned above. We use periodic boundary conditions with a range of linear system sizes  $L = 24$  to  $60$ . For  $L = 60$ , the system contains  $N = 2600$  background disks at a density of  $\phi = 0.8395$ .

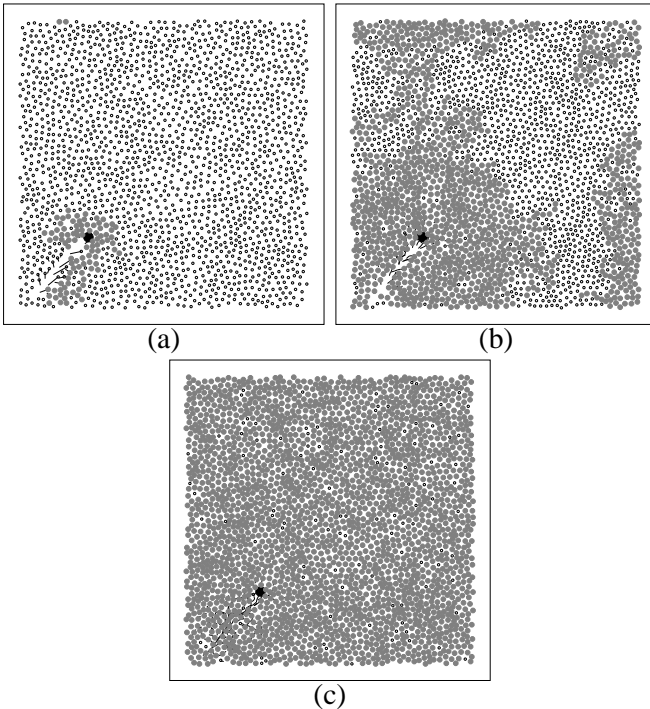


FIG. 1. Sample geometry for  $L = 60$  and (a)  $\phi = 0.656$ , (b)  $\phi = 0.811$ , (c)  $\phi = 0.837$ . Large black dot: the probe disk (size exaggerated for clarity); gray dots: moving disks; small dots: non-moving disks.

We prepare the system by randomly dropping nonoverlapping disks up to  $\phi \approx 0.6$ . To reach higher densities, we add disks at randomly selected interstitial locations, reduce the radii of all disks, and then increase the radii back to the initial values while allowing the system to evolve under a small temperature. This produces nonoverlapping configurations at densities up to  $\phi_c$ . To reach the maximum possible density,  $\sqrt{3}\pi/6 \approx 0.907$ , requires phase separating the system. At the significantly lower  $\phi_c \approx 0.839$  we find no phase separation. Since the system is not jammed below  $\phi_c$ , we believe that we successfully uniformly sampled all available states, and that phase separation does not occur until some  $\phi_{sep} > \phi_c$ .

To study the velocity curve, we drive a single large disk along a  $45^\circ$  angle over a distance of  $\sqrt{2}L/5$ . The time required for this motion is much longer than the time scale of any brief initial transients in the velocity. We measure the effective velocity of the driven disk over the length of the simulation. For computational reasons, it is not possible to simulate a disk moving at an arbitrarily slow velocity through the system. In these cases, we declared that the system had jammed; this definition agreed well with the critical  $\phi_c \approx 0.839$  given by curve fitting below.

In Fig. 1 we show snapshots of simulation results for different densities, with disks counted as moving and shaded in gray if they were connected via a force contact to the driven disk. At the lowest  $\phi = 0.656$ , in Fig. 1(a), the driven disk moves easily and interacts with only a

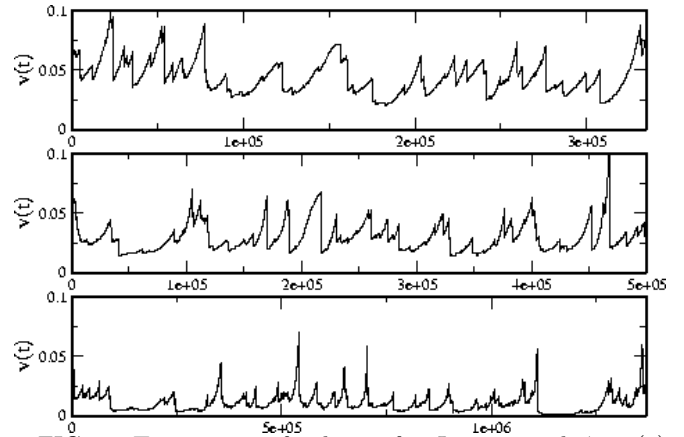


FIG. 2. Time series of velocity for  $L = 60$  and  $\phi =$  (a) 0.656, (b) 0.747, and (c) 0.837.

few neighbors. In Fig. 1(b) for  $\phi = 0.811$ , close to jamming, a larger portion of the disks are moving, while in Fig. 1(c) at  $\phi = 0.837$ , the system is sufficiently close to  $\phi_c$  that the entire (finite-size) sample is moving.

Figure 2 shows example time series for the velocity  $v$  parallel to the applied drive at  $\phi = 0.656$ , 0.747, and 0.837. Not only does the average velocity decrease as  $\phi$  increases, but the time series becomes more intermittent. At  $\phi = 0.837$ , the velocity is usually very small, but there are occasional bursts of much higher velocity.

We emphasize that for  $\phi < \phi_c$  the threshold force required to move the driven particle vanishes. Instead,  $v$  is proportional to the drive  $f_d$  at any moment of time. This follows from dimensional grounds, since for a hard-core system, there is no physical parameter with units of force. This is very different from the behavior shown in a recent numerical study of single probe particles driven through a system with softer, long-range forces [7], where there is a non-vanishing, but finite, depinning force at all densities due to the long-range nature of the force.

*Distribution of Velocities*— Newton's third law, combined with Eq. (1), leads to the result that  $\eta \sum_i \mathbf{v}_i = \mathbf{f}_d$ . Thus, if the driven particle is not in contact with any other particles, it moves at  $v = f_d/\eta$ . If there are a total of  $n$  particles moving together, including the driven particle, then they each move at  $v = f_d/n$ . For  $\phi > \phi_c$ , all  $N$  particles in the system move together, and  $v$  is vanishingly small in the thermodynamic limit. For  $\phi < \phi_c$ , the number of particles moving is finite in the thermodynamic limit and diverges as  $\phi$  approaches  $\phi_c$ .

One measurement which may show scaling as  $\phi$  approaches  $\phi_c$  is the average velocity  $v$  of the driven disk. However,  $v$  is a random, time-dependent variable, and for any density  $\phi < \phi_c$  there is a nonvanishing probability of observing any given, arbitrarily small  $v$ . Since the other disks are distributed randomly, there is still some probability that in any local region the density will exceed  $\phi_c$  [8] (this argument is inspired by Lifshitz tails). If this region encloses  $n$  disks, the probability of finding such a

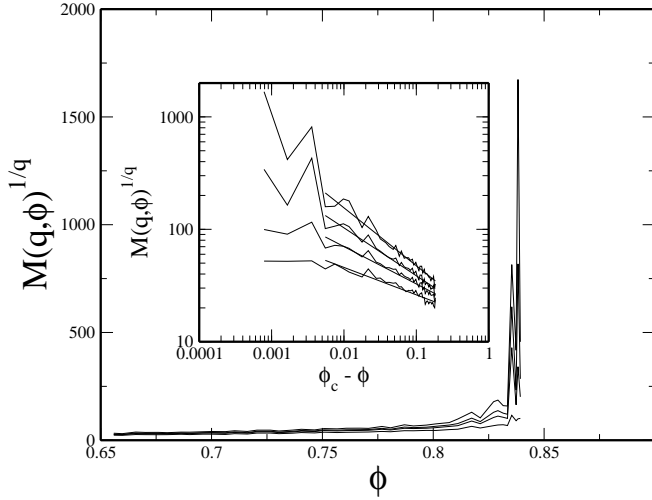


FIG. 3. Plot of  $M(q, \phi)^{1/q}$  versus  $\phi$  for  $q = -1, 1, 2$ , and  $4$  (from bottom to top). The curves with larger  $q$  are noisier. Inset:  $M(q, \phi)^{1/q}$  versus  $\phi_c - \phi$  on a log-log scale for  $q = -3, -1, 1, 3$ . A curve fit shows the power law scaling.

region is exponentially small in  $n$ , but it is nonvanishing. When the driven disk hits such a region, it behaves as if it jams, and  $v$  slows to a value of order  $1/n$  until the disk either escapes the region or pushes other disks into neighboring regions of lower density. Thus, with exponentially small probability in  $n$ ,  $v \sim O(1/n)$ . Once the particle slows, however, it takes a long time for it to leave the region. Thus, one expects to see an intermittent  $v$ .

To measure the intermittency, we use multifractal [9] scaling. For a given  $\phi$ , let  $p(v)dv$  be the probability of measuring a given  $v$  at a single instant in time. Define the  $q$ -th inverse moment by  $M(q) = \int dv p(v) v^{-q}$  as the time average of the  $q$ -th power of the inverse velocity. We then define a set of multifractal exponents  $\tau(q)$  by

$$M(q) = \int dv p(v) v^{-q} \propto (\phi_c - \phi)^{-\tau(q)}. \quad (2)$$

If  $v$  were constant throughout the simulation for a given  $\phi$ , we would have  $M(q)^{1/q} = M(1)$ . If instead  $v$  had relative fluctuations of order unity about some characteristic velocity,  $v_0(\phi)$ , then  $M(q)^{1/q}$  would not equal  $M(1)$  in general, but  $\tau(q)/q$  would still be independent of  $q$ . We will instead find that  $\tau(q)/q$  depends on  $q$ . This implies that  $v$  does not simply fluctuate about a single  $v_0$ , but is instead much more intermittent, with the particle sometimes getting stuck for a long time at a slow velocity, then traveling much more rapidly.

We compute the moments  $M$  and extract the exponents  $\tau(q)$  by fitting the moments to the form  $c * (\phi_c - \phi)^{-\tau(q)}$ . The value of  $\phi_c$  determined from these fits is independent of  $q$  to high accuracy for  $q \geq -2$ , and thus we can fix  $\phi_c \approx 0.839$  as the onset of jamming. In Fig. 3 we plot  $M(q, \phi)^{1/q}$  versus  $\phi$  for  $L = 60$  and various  $q$ , averaged over three realizations of the system. In the inset we show the log-log plot of the curves in the main panel

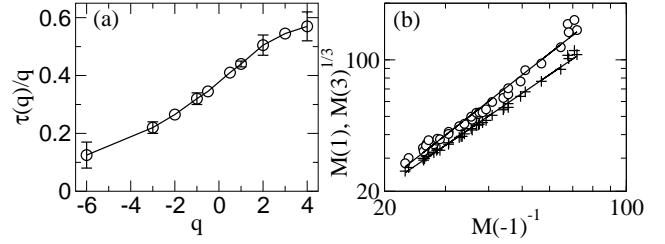


FIG. 4. (a): Plot of  $\tau(q)/q$  against  $q$ . The  $q$  dependence of  $\tau(q)/q$  shows the existence of multiscaling in this system. (b): Plot of  $M(1)$  (crosses) and  $M(3)^{1/3}$  (circles) against  $M(-1)^{-1}$ .

with solid lines indicating power law fits. The curves not only fail to overlap, but also have different slopes, indicating the presence of multiscaling. In Fig. 4(a), we plot  $\tau(q)/q$  versus  $q$ . For large positive and negative  $q$ , the plot asymptotes. The asymptote at large positive  $q$  reflects the scaling of the typical (disregarding exponentially rare possibilities discussed above) slowest velocity of the system which goes to zero as  $(\phi - \phi_c)^{\lim_{q \rightarrow \infty} \tau(q)/q}$ . Similarly, the asymptote at negative  $q$  reflects the typical largest velocity. Since  $\lim_{q \rightarrow -\infty} \tau(q)/q$  is very close to zero, the typical largest velocity is largely independent of  $\phi$ , as seen in Fig. 2. In fact, it is likely that at sufficiently negative  $q$  the exponent  $\tau(q)/q$  becomes zero.

The error in  $\tau(q)$  due to statistical fluctuations is negligible. If we compare the  $\tau(q)$  obtained by curve fitting  $M(q, \phi)$  averaged over all realizations to  $\tau(q)$  obtained by using only a single realization, the difference in exponents is of order 0.001 to 0.002. Instead, the major source of error is finite size effects. The straight lines in the inset to Fig. 3 are based on fitting over a certain range of  $\phi$ . For  $\phi$  closer to  $\phi_c$  than the endpoint of the fitting lines, the statistical noise in the data increases significantly and some of the realizations jam while others do not. Thus, for finite  $N$  the jamming threshold is not well defined, and these  $\phi$  are so close to  $\phi_c$  that finite size effects may be important. The error bars in Fig. 4 are based on this consideration of finite size effects. The low end of the error bars corresponds to the  $\tau(q)$  obtained by fitting only over the range shown in the inset to Fig. 3, while the high end corresponds to including all  $\phi < \phi_c$ . The low end tends to underestimate the difference in  $\tau(q)/q$  for different  $q$ .  $\tau(q)/q$  is clearly  $q$ -dependent since the difference in  $\tau(q)/q$  between  $q = -1$  and  $q = 2$ , for example, is definitely outside the error bars. In Fig. 4(b) we plot  $M(q)^{1/q}$  as a function of  $M(-1)^{-1}$  for  $q = 1, 3$  over the same range as in Fig. 3 to illustrate that the data obey extended self-similarity [10]. The slopes on the log-log plot are  $1.25 \pm 0.15$  and  $1.45 \pm 0.2$  respectively; as expected, this is within error bars of the ratio of the exponents  $-\tau(1)/\tau(-1)$  and  $-(\tau(3)/3)/\tau(-1)$ . It is difficult to establish that these slopes are different from each other, but the slopes are definitely different from unity, which already indicates multiscaling. The fact that  $\tau(-1)$  is

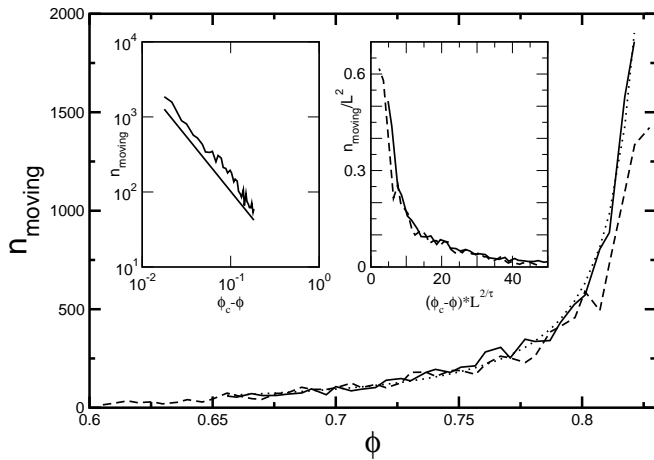


FIG. 5. Plot of  $n_{\text{moving}}$  against  $\phi$ . Solid line:  $L = 60$ . Dashed line:  $L = 48$ . Dotted line: a power law fit to the  $L = 60$  curve. Left inset: The  $L = 60$  curve and the fit against  $\phi_c - \phi$ , showing scaling. Right inset: finite size scaling.

less than one makes the size of the scaling regime seem small, since a wide scaling range in  $\phi$  leads to only a small range in  $M(-1)$ ; however, the curve fit is very good over the available range.

Figure 1 shows that as the jamming transition is approached, the number of moving disks increases and there is a diverging length scale as the jamming is approached. In order to quantify this, we show in Fig. 5 the number of moving disks  $n_{\text{moving}}$  vs  $\phi$  for systems of linear size  $L = 48$  and  $L = 60$ . Here a clear divergence appears as the critical density is approached. The divergence is cut off when  $n_{\text{moving}}$  equals the total number of disks. We have also considered smaller systems for different parameters of drive and disk radii and again observe a divergence; however, these smaller systems give a much lower resolution and hence a larger error on the estimated exponent. In Fig. 5 we fit a power law to the largest system with  $(\phi_c - \phi)^\tau$ , where  $\tau$  is between 1.2 and 1.46. We also measured the sum over moving disks of the squared distance between the driven disk and the moving disk, a quantity  $n_{\text{moving}}l^2$ , and find that this number diverges as  $(\phi_c - \phi)^{-\sigma}$ , with  $\sigma$  between 2.35 and 2.6. The number of moving disks cannot directly be compared to the velocity  $v$  of the driven disk, as the driven disk can push other disks normal to the drive so that  $n_{\text{moving}}$  may be much larger than  $1/v$ . We obtained the exponents  $\tau$  and  $\sigma$  by a time average of the number of moving disks, and did not perform a multiscaling calculation, though we can extract a length from a simple scaling analysis. If the moving disks form a cluster with dimension  $d$  and length scale  $\xi$  diverging as  $\xi \propto (\phi_c - \phi)^{-\nu}$ , then  $\tau = \nu d$  and  $\sigma = \nu(d + 2)$ . Given the values of  $\tau$ ,  $\sigma$ , and our own qualitative observations, we find  $d = 2$ , so that  $\nu$  is between 0.6 and 0.7. This provides a direct measurement of the diverging length scale, in reasonable agreement with the finite-size scaling result [3]  $\nu = 0.71 \pm 0.12$ . We

note that Fig. 5 in our case is completely consistent with finite-size scaling as shown in the right inset. Scale the  $y$ -axis by  $L^2$  (the scaling for the total number of particles in the system), and scale  $\phi_c - \phi$  by  $L^{-2/\tau}$ . Then, the curves for different  $L$  automatically collapse within the scaling region, and since the divergence is cutoff at  $n_{\text{moving}} \propto L^2$  for all  $L$ , these curves also collapse close to  $\phi_c$ . Finally, our  $\phi_c \approx 0.839$  is very close to the critical packing density found in [3].

*Conclusion*— We have studied a system of a  $T = 0$ , zero shear 2D disordered assembly of disks at densities below and up to Point J in the recently proposed jamming phase diagram. A single probe disk is pushed with a constant drive through the other disks. Upon increasing the packing density, we find a jamming transition associated with a power law divergence in the number of moving disks and a diverging spatial correlation length, indicating that Point J is a true continuous phase transition. In addition, we show that the tails of the disk velocity distribution play an important role in this transition, since due to the non-thermal nature of the system, once the particle stops moving, it cannot restart. Using the multifractal moments  $\tau(q)$ , we chart the tails and show that the  $\tau(q)$  do not depend linearly on  $q$ ; thus, the system exhibits multiscaling. We also find evidence for a diverging correlation length of the force contacts as the jamming transition is approached from below. Our results show that there is an underlying *second order* non-thermal phase transition at the jamming transition. We suggest that experimental work should consider both the velocity time series and the number of moving particles in the surrounding media, and should test for multiscaling behavior as the jamming transition is approached. Particular experiments would include driving a single disk on a flat surface through a disordered assembly of other disks for increasing density, or driving individual colloids through glassy assemblies of other colloids.

*Acknowledgments*— We thank E. Weeks for useful discussions. This work was supported by the U.S. DOE under Contract No. W-7405-ENG-36.

- 
- [1] *Jamming and Rheology* ed. A. J. Liu and S. R. Nagel (Taylor & Francis, N. Y., 2001).
  - [2] A.J. Liu and S.R. Nagel, *Nature (London)* **396** 21 (1998).
  - [3] C. S. O'Hern *et al.*, *Phys. Rev. E* **68**, 011306 (2003).
  - [4] S. N. Coppersmith *et al.*, *Phys. Rev. E* **53**, 4673 (1996).
  - [5] H.J. Herrmann, *Int. J. Mod. Phys. C* **4**, 309 (1993).
  - [6] P. Habdas, D. Schaar, A. C. Levitt, and E. R. Weeks, *Europhys. Lett.* **67**, 477 (2004).
  - [7] M. B. Hastings, C. J. Olson Reichhardt, and C. Reichhardt, *Phys. Rev. Lett.* **90**, 098302 (2003).
  - [8] I. M. Lifshitz, *Sov. Phys. JETP* **17**, 1159 (1963).
  - [9] T. C. Halsey *et al.*, *Phys. Rev. A* **33**, 1141 (1986); H. G. E. Hentschel and I. Procaccia, *Physica D* **8**, 435 (1983).
  - [10] R. Benzi *et al.*, *Phys. Rev. E* **48**, R29 (1993).